J. Fluid Mech. (2011), *vol.* 675, *pp.* 518–528. © Cambridge University Press 2011
doi:10.1017/jfm.2011.117

Localisation of convection in mushy layers by weak background flow

S. M. ROPER[1]†, S. H. DAVIS[2] AND P. W. VOORHEES[3]

[1]School of Mathematics and Statistics, University of Glasgow, Glasgow G12 8QW, UK
[2]Engineering Sciences and Applied Math, Northwestern University, Evanston, IL 60208-3125, USA
[3]Materials Science and Engineering, Northwestern University, Evanston, IL 60208-3108, USA

(Received 25 October 2010; revised 4 February 2011; accepted 4 March 2011)

It is known that freckles form at the sidewalls of directionally solidified materials. We present a weakly nonlinear analysis of the effects of a weak and slowly varying background flow formed by non-axial thermal gradients on convection near onset in a mushy layer. We find that in the two-dimensional case, the onset of mush convection occurs away from the walls. However if three-dimensional disturbances are allowed, the onset occurs near the walls of the container confining the mush. We derive amplitude equations governing this behaviour and simulate their evolution numerically.

Key words: convection in porous media, low-dimensional models, solidification/melting

1. Introduction

Many machine parts are cast from multi-component metallic alloys. When the liquid alloy cools, the liquid–solid interface can become unstable (Mullins & Sekerka 1964) and form dendrites. The dendrites plus the interstitial fluid, the *mushy layer* (e.g. Fowler 1985; Worster 1992), are further susceptible to convective instabilities that can result in the formation of *chimneys* – dendrite free regions that are observed in the frozen sample as defects called freckles (e.g. Madison *et al.* 2008). In extended systems, chimneys may form a spatially periodic array. However, casting engineers have noted that in moulds, necessarily of finite extent, these defects are seen preferentially near the mould walls (Giamei & Kear 1970). The mould walls are the site of heat transfer to the exterior of the mould. Such heat transfer deforms the isotherms and creates horizontal temperature gradients. These gradients excite all modes of mush convection, including a convective mode on the scale of the mould and the most unstable mush-mode (Worster 1992). The effect of an excitation of the mush-mode is to modify the bifurcation to convection such that it becomes *imperfect* (Impey, Riley & Winters 1990). The effect of the mould-scale convective mode on the mush-mode near onset is explored in this paper.

Modelling the behaviour of the mushy layer involves a description of transport and generation of heat, solute and momentum in the liquid and the mush (e.g. Hills, Loper & Roberts 1983; Worster 1997). The mush is usually described as a reactive porous medium. A mush in which the solid and liquid are in local thermodynamic

† Email address for correspondence: Steven.Roper@glasgow.ac.uk

https://doi.org/10.1017/jfm.2011.117 Published online by Cambridge University Press

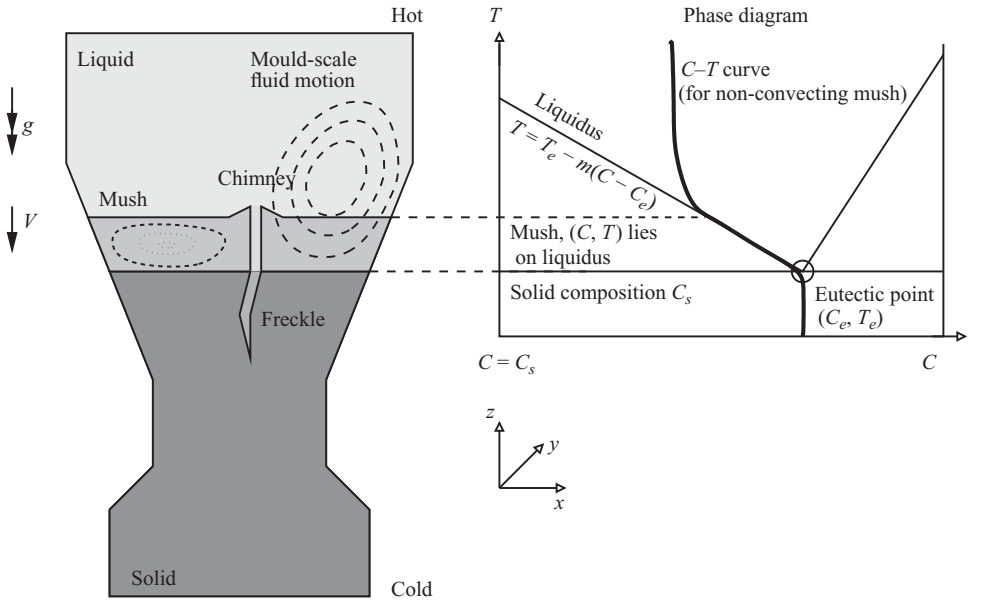


FIGURE 1. Directional solidification of a multi-component alloy can lead to the development of a mushy zone and freckles. A mould filled with liquid alloy is pulled through a temperature gradient, the mould is generally not of constant cross-section, nor adiabatic and a circulation on the scale of the mould is induced. At equilibrium, the phases present at a given temperature T and composition C are described by the phase diagram, shown here for a binary eutectic alloy.

equilibrium is called an *ideal* mush. The thermodynamic phase diagram of the alloy indicates which phases are present at a given temperature and composition and controls the structure of the mush. In particular, the equations that describe *directional solidification*, in which a liquid sample is solidified by pulling it at constant speed V through a thermal gradient, admit a steady state solution in which a mushy layer separates liquid and solid. A model for the mush must include a description of its permeability and how the density of interstitial fluid varies with temperature and composition. The stability of the steady state depends on the mush Rayleigh number R_m, constructed from the mush permeability, buoyancy variation, viscosity and depth. When the mush Rayleigh number is near a critical R_c, there is a bifurcation to a convecting state, the nonlinear evolution of which leads to the formation of chimneys (e.g. Schulze & Worster 1999; Katz & Worster 2008).

Weak lateral heat transport (compared to heat transported by the pulling speed V) at the mould walls (see figure 1) creates a horizontal gradient in buoyancy that causes a circulation on the scale of the mould. If the mush is much thinner than the scale of the mould (as we consider in this paper), the effect of a weak heat loss at the mould walls is to introduce a weak circulation on a scale much larger than that of the mush-mode of convection. The basic state then has a steady background circulation. As well as introducing transport the background flow modifies the thermodynamic conditions in the mush. We separate these effects and consider a model problem in which we explore the effect of a weak and large-scale background flow on the mush-mode of convection for a thin and isolated mushy layer. We propose a mechanism for why chimneys might be expected to form at or near the mould walls of a directionally solidified sample. We use weakly nonlinear analyses to understand

https://doi.org/10.1017/jfm.2011.117 Published online by Cambridge University Press

how this localisation might take place. In § 2, we discuss the governing equations, followed by a discussion of convenient limits for our analysis in § 3. The effect of a weak background flow is examined in § 4.

2. Governing equations

The equations used to describe convection in an ideal mushy layer are well established in the literature (e.g. Fowler 1985; Worster 1992; Amberg & Homsy 1993) and are presented here for completeness. A binary alloy is pulled at speed V towards a cooled region (see figure 1). The temperature of the fluid as $z \to \infty$ is T_∞ and its far-field composition is C_0. At a temperature $T = T^*$ the fluid becomes completely solid and a partially solidified mush region extends over $T^* < T < T_i$, where T_i is the temperature at the mush–liquid interface. In our case, T^* is the eutectic temperature T_e, below which the sample is completely solid.

The temperature T and composition C of the liquid satisfy advection–diffusion equations. In a frame fixed in the lab, we write the fluid velocity as $\boldsymbol{u} - V\boldsymbol{k}$, where $\boldsymbol{u}$ is the fluid velocity additional to that due to the pulling of the sample. In the mush $\boldsymbol{u}$ is the Darcy velocity. The fluid velocity, $\boldsymbol{u} - V\boldsymbol{k}$, satisfies the Navier–Stokes equations in the liquid and $\boldsymbol{u}$ satisfies Darcy's law in the mush. The phases of the alloy that are present for a particular temperature and composition is described by the phase diagram (a typical phase diagram for a eutectic alloy is shown in figure 1), we assume that the liquidus is given by $T_L(C) = T_e - m\,(C - C_e)$, where T_e, C_e and m are the eutectic temperature, eutectic composition and liquidus slope, respectively (see figure 1). Conservation of solute applies in the mush and it is assumed that the fluid in the mush is in local equilibrium with the solid, that the fluid is well-mixed in the pores and that, within the solid, solute diffuses faster than any time scale of interest, so that the liquid and solid are in local equilibrium and the liquid temperature and composition are constrained to lie on the liquidus. We assume that the thermophysical properties of the solid and liquid phases in the mush are the same, so that average thermophysical properties of the mush are the same as for the individual solid and liquid phases.

The mush is described by a solid fraction ϕ and an isotropic permeability $\Pi(\chi)$, where $\chi = 1 - \phi$ is the liquid fraction. The permeability has scale Π_0. We assume that the solid phase has constant composition C_s. Denote the far-field composition as C_0. The temperature scale is $\Delta T = T_L(C_0) - T_e$ and the composition scale is $\Delta C = C_e - C_0$. Remaining quantities that describe the system are the pressure p, the diffusivities of temperature κ and of composition D, the dynamic viscosity μ, the latent heat of fusion per kilogram L and the specific heat C_p. The density is $\rho(T, C)$ and a reference density is ρ_0. The kinematic viscosity is $\nu = \mu/\rho_0$. The Boussinesq approximation is made so that density variations are retained only in the buoyancy terms in the Navier–Stokes equation. The thermal expansion coefficient, at the reference density ρ_0, is α^* and the solutal expansion coefficient is β^*. Gravity $\boldsymbol{g} = -g\boldsymbol{k}$ points downwards, in the direction in which the sample is being pulled.

The non-dimensional parameters that control the behaviour of the system are the Lewis number $Le = \kappa/D$, Prandtl number $\sigma = \nu/\kappa$, inverse Darcy number $\mathscr{H} = \kappa^2/V^2\Pi_0$, $\mathscr{A} = \alpha^*\Delta T/\beta\Delta C$ (where β is an expansion coefficient in the mush that combines the effects of temperature and composition, $\beta = \beta^* + \alpha^* m$), mush Rayleigh number $R_m = g\beta\Delta C\Pi_0/V\nu$, Stefan number $\mathscr{S} = L/C_p\Delta T$ and compositional number $\mathscr{C} = C_0/\Delta C$. The far-field boundary condition for temperature gives another non-dimensional parameter $\theta_\infty = [T_\infty - T_L(C_0)]/\Delta T$.

https://doi.org/10.1017/jfm.2011.117 Published online by Cambridge University Press

2.1. *Non-dimensionalisation*

The non-dimensionalised equations for an ideal mushy layer with an overlying liquid layer are (from Worster 1992)

$$\frac{\partial \theta}{\partial t} - \frac{\partial \theta}{\partial z} + \boldsymbol{u}\cdot\nabla\theta = \nabla^2\theta, \tag{2.1}$$

$$\frac{\partial \Theta}{\partial t} - \frac{\partial \Theta}{\partial z} + \boldsymbol{u}\cdot\nabla\Theta = \frac{1}{Le}\nabla^2\Theta, \tag{2.2}$$

$$\frac{1}{\sigma}\left(\frac{\partial \boldsymbol{u}}{\partial t} - \frac{\partial \boldsymbol{u}}{\partial z} + \boldsymbol{u}\cdot\nabla\boldsymbol{u}\right) = R_m\mathscr{H}\mathscr{A}\theta\boldsymbol{k} - R_m\mathscr{H}(1+\mathscr{A})\Theta\boldsymbol{k} - \mathscr{H}\nabla p + \nabla^2\boldsymbol{u}, \tag{2.3}$$

in the liquid and

$$\frac{\partial \theta}{\partial t} - \frac{\partial \theta}{\partial z} + \boldsymbol{u}\cdot\nabla\theta = \nabla^2\theta + \mathscr{S}\left(\frac{\partial \phi}{\partial t} - \frac{\partial \phi}{\partial z}\right), \tag{2.4}$$

$$\left(\frac{\partial}{\partial t} - \frac{\partial}{\partial z}\right)[(\mathscr{C}-\Theta)(1-\phi)] + \boldsymbol{u}\cdot\nabla\Theta = 0, \tag{2.5}$$

$$\theta = \Theta, \tag{2.6}$$

$$\boldsymbol{u} = -\Pi(\chi)(\nabla p + R_m\theta\boldsymbol{z}), \tag{2.7}$$

in the mush. In both liquid and mush, the fluid is incompressible so that

$$\nabla\cdot\boldsymbol{u} = 0. \tag{2.8}$$

The non-dimensional temperature and composition are defined by

$$\theta = \frac{T - T_L(C_0)}{\Delta T}, \quad \Theta = \frac{C_0 - C}{\Delta C}. \tag{2.9}$$

Equations (2.1)–(2.7) represent: advection and diffusion of heat in the liquid (2.1); advection and diffusion of solute in the liquid (2.2); Navier–Stokes momentum equation in the liquid (2.3); advection, diffusion and generation of heat by solidification in the mush (2.4); conservation of solute in the mush (2.5); constraint that liquid is in equilibrium with solid in the mush, i.e. that temperature is slaved to concentration via the liquidus relation (2.6); Darcy's law for fluid flux in the mush (2.7). In order to arrive at these equations, dimensional lengths have been scaled with κ/V, time with κ/V^2, velocities with V and pressure with $\kappa\mu/\Pi_0$. By virtue of the liquidus, the linear equation of state in the mush becomes

$$\rho = \rho_0(1 + \beta^*\Theta\Delta C - \alpha^*\theta\Delta T) = \rho_0(1 + \beta\theta\Delta C). \tag{2.10}$$

Equations (2.1)–(2.7), with appropriate boundary conditions, can be solved to give the steady non-convecting solution. The structure of the steady solution is characterised by the set of non-dimensional parameters $(Le, \mathscr{S}, \mathscr{C}, \theta_\infty, \mathscr{A}, \mathscr{H}, R_m)$, together with any non-dimensional parameters that may be derived from boundary conditions and the mush depth. This same set of parameters also determine the stability of the steady solution to convective motions.

In this paper, we are concerned with the effects of a weak background flow on the amplitude of weakly nonlinear mushy-layer convection. These effects can be studied using simplified model problems which capture the effect of a weak background flow.

https://doi.org/10.1017/jfm.2011.117 Published online by Cambridge University Press

3. Limits

It has been shown (Amberg & Homsy 1993) that in the limit of large far-field temperature, the mushy layer is much thinner than the scale κ/V, set by the pulling speed and thermal diffusion. The non-dimensional mushy layer depth in this case is given to leading order as $h=\delta\sim\theta_\infty^{-1}\ll 1$. This result motivates a further rescaling of the variables. Following Amberg & Homsy (1993) and Anderson & Worster (1995), we remove any large effects of compositional changes on the solid fraction by assuming the compositional number is large $\mathscr{C}=\bar{C}/\delta$ (the near-eutectic approximation) and that therefore the solid fraction is $\phi\sim O(\delta)$, from (2.5). Similarly, we can retain the effects of latent heat by scaling the Stefan number $\mathscr{S}=\bar{S}/\delta$. The barred quantities are assumed $O(1)$. We scale lengths with the mush depth δ. The Rayleigh number is written in terms of the mush depth as $R_m=R^2/\delta$, and time is scaled by δ^2.

Using the same expansion as Anderson & Worster (1995), we expand perturbation variables in a double power series in ϵ (the strength of the background flow) and δ (the non-dimensional mush depth), so that a general quantity q is written as

$$q=q_B+\tilde{q}=q_B+\epsilon\sum_{n=0}^{\infty}\epsilon^n\sum_{m=0}^{\infty}\delta^{k_n^q}\delta^m q_{nm},\quad\text{with }\epsilon\ll\delta\ll 1. \tag{3.1}$$

Here the integers k_n^q (the superscript q refers to the quantity under consideration) are needed to ensure the correct balance between terms in the governing equations (in particular $k_0^\phi=k_1^\phi=0$ and $k_2^\phi=-1$, and $k_i^q=0$, $i=0,1,2$ for other quantities, see Anderson & Worster 1995). Define a slow time scale $\tau=\epsilon^2 t$ and a slow space scale $X=\epsilon x$. Insertion of (3.1) into (2.4)–(2.7) yields new governing equations for the variables q_{nm}.

Throughout the analysis, we use the rigid-lid assumption (Amberg & Homsy 1993; Anderson & Worster 1995) so that the mush–liquid interface remains at $z=1$ and the boundary conditions for the perturbation quantities at the mush–solid ($z=0$) and mush–liquid interfaces are the same at all orders,

$$\tilde{w}(x,y,0)=\tilde{w}(1)=\tilde{\theta}(0)=\tilde{\theta}(1)=\tilde{\phi}(1)=0. \tag{3.2}$$

This simplification allows us to consider a mushy layer that is isolated from the overlying liquid layer. In this manner, we reduce the set of governing equations to those only in the mush.

4. Localisation by a weak background flow

An effect of lateral heat transport at the mould walls is to induce a large-scale background flow in the liquid and mush, on the scale of the container (figure 1). In general, the lateral heat transport excites convection at all allowable wavenumbers in the mushy layer, including the mush-mode and a mode on the scale of the domain. If the lateral transport of heat is a small perturbation to the steady state of directional solidification, the flow induced in the mushy layer will be weak. In general this background flow will involve a modification to both the liquid and the mush as shown on the right of the figure 1, its form will depend on the full set of non-dimensional parameters (Le, $\mathscr{S}$, $\mathscr{C}$, θ_∞, $\mathscr{A}$, $\mathscr{H}$, R_m). For the purposes of our analysis, we assume that the background flow induced by the sidewall heat transfer produces a modification in the mushy layer only (figure 1*a*) and continue to use the rigid-lid approximation; this is appropriate in cases where the thermal buoyancy in the liquid acts to confine motions in the mush, as discussed in Chung & Chen (2000).

https://doi.org/10.1017/jfm.2011.117 Published online by Cambridge University Press

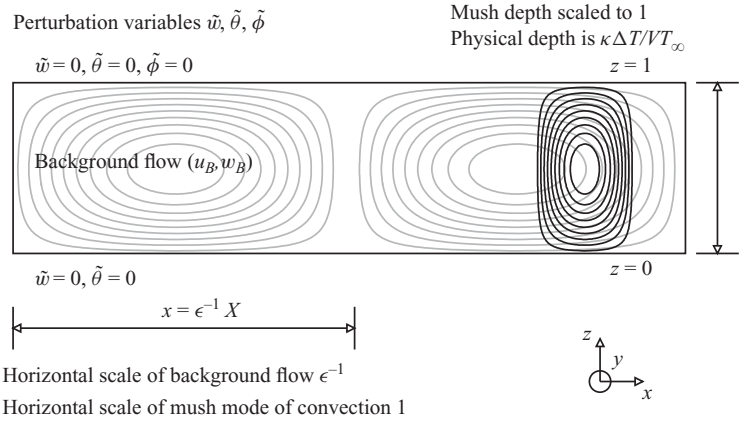


FIGURE 2. The domain used for the weakly nonlinear analysis is scaled so that the background flow varies on the scale ϵ^{-1}, the mush depth is 1 and the mush-mode of convection has a horizontal scale that is $O(1)$.

A summary of the mathematical domain, with representative scales, is provided in figure 2. The governing equations are those in § 3, with a non-zero background flow $\boldsymbol{u}_B = (u_B, w_B)$, for example

$$w_B = \epsilon^3 P \sin \pi z \cos \epsilon\alpha x, \quad u_B = -\epsilon^2 \frac{P\pi}{\alpha} \cos \pi z \sin \epsilon\alpha x, \tag{4.1}$$

where P is a constant measure of the intensity of the background flow. The form of (4.1) could be regarded as the excitation of a mode of convection with horizontal wavenumber $\epsilon\alpha$ by sidewall heat transfer. The horizontal component of background flow u_B is zero at locations $\epsilon\alpha x = j\pi$ with $j \in \mathbb{Z}$ where we imagine idealised (planar with slip) walls of the mould to be placed. We may also imagine the background flow as generated by a slow variation in the distribution of pressure at the top of the mushy layer, which arise as a result of fluid motion in the liquid layer; a variation in pressure at $z=1$ causes horizontal flow in the mushy layer. For example, the steady background flow and associated temperature field when the pressure at $z=1$ is $O(\epsilon)$ and varies on the scale ϵ^{-1} at $O(\delta^0)$ is

$$w_B = -\epsilon^3 U'(X) z, \quad u_B = \epsilon^2 U(X), \quad \theta_B = 1 - z + \frac{\epsilon^3}{6}(z^3 - z)U'(X), \tag{4.2}$$

where $X = \epsilon x$, the slow space scale, and $U(X)$ is determined by the dynamics in the liquid layer. Through insertion of (3.1) for the quantities θ, ϕ, u and w into the governing equations (2.1)–(2.10) and examination at each order in ϵ and δ yields the equations for various orders of ϵ and δ. In particular (see Anderson & Worster 1995) at $O(\epsilon^1\delta^0)$ the convection is described by the marginally stable mode in an infinite horizontal system with an amplitude $A(X, \tau)$ modulated by the slow space and time scales X and $\tau = \epsilon^2 t$. For the marginally stable mode, the wavenumber k_c and scaled Rayleigh number R_c are given by $k_c = \pi$, and $R_c = 2\pi\Omega^{-1/2}$. The corresponding velocity, temperature and solid fraction are given by

$$\boldsymbol{q}_{00} = [w_{00}, u_{00}, v_{00}, \theta_{00}, \phi_{00}] = A(X, \tau)\left[\sin \pi z, \mathrm{i}\cos\theta \cos \pi z, \mathrm{i}\sin\theta \cos \pi z, -\frac{\Omega \sin \pi z}{2\pi}, -\frac{2(1+\cos \pi z)}{\Omega^{1/2} C}\right] \mathrm{e}^{\mathrm{i}\boldsymbol{k}\cdot\boldsymbol{x}} + \text{c.c.}, \tag{4.3}$$

https://doi.org/10.1017/jfm.2011.117 Published online by Cambridge University Press

where $\boldsymbol{k} = \pi(\cos\theta, \sin\theta)$. The constant $\Omega = 1 + \bar{S}/\bar{C}$ combines the effects of latent heat and composition. The constants K_1 and K_2 that appear in the equations are related to the permeability $\Pi(1-\phi)^{-1} \approx 1 + K_1\phi + K_2\phi^2 + \cdots$. The background flow is initially written using (4.1) with $P \sim O(1)$. The angle θ is the angle between the roll-axis and y-axis. Rolls with $\theta = \pi/2$ are called longitudinal rolls and $\theta \neq \pi/2$ are oblique rolls, rolls with $\theta = 0$ are two-dimensional rolls. For longitudinal rolls, we rescale the background flow (Chen & Davis 1999) so that the background flow interacts with the convection at $O(\epsilon^2)$ (otherwise the interaction is at $O(\epsilon^3)$). The background flow for longitudinal rolls is modified to

$$w_B = \epsilon^2 P \cos\alpha X \sin\pi z, \qquad u_B = -\epsilon \frac{P\pi}{\alpha} \sin\alpha X \cos\pi z, \tag{4.4}$$

where $X = \epsilon x$, the slow spatial scale, so that the background flow interacts with the convection at $O(\epsilon^3)$.

Upon application of solvability conditions at $O(\epsilon^3\delta^0)$ (using the solution of the adjoint problem at $O(\epsilon^1\delta^0)$), the following amplitude equations are derived. For oblique rolls, the amplitude of the convection is governed by

$$\left(\Omega - 2\frac{S}{C^2\Omega}\right)\frac{\partial A}{\partial \tau} = 2A_{XX}\cos^2\theta + \left(2\pi R_2 \Omega^{1/2} - 2\pi^2 \frac{K_1 P}{C\Omega^{1/2}} i \sin\alpha X \cos\theta\right) A + \pi^2 |A|^2 A \left(\frac{64K_1^2}{3\Omega C^2} + \frac{4K_1}{C} - 2\Omega - \frac{22K_2}{\Omega C^2}\right) \tag{4.5}$$

and for longitudinal rolls the amplitude equation is

$$\left(\Omega - 2\frac{S}{C^2\Omega}\right)\frac{\partial A}{\partial \tau} = \left(2\pi R_2 \Omega^{1/2} - 8\pi\alpha \frac{K_1 P}{C\Omega^{1/2}} \cos(\alpha X)\right) A - 2\pi \frac{K_1 P}{C\Omega^{1/2}} \sin(\alpha X) \frac{\partial A}{\partial X} + \pi^2 |A|^2 A \left(\frac{64K_1^2}{3\Omega C^2} + \frac{4K_1}{C} - 2\Omega - \frac{22K_2}{\Omega C^2}\right). \tag{4.6}$$

The coefficients of $|A|^2 A$ and $\partial A/\partial\tau$ are precisely those found in Anderson & Worster (1995). Both equations can be generalised to include variations along the rolls; for example in (4.5) with $\cos\theta = 1$ the term $2A_{XX}$ becomes $2(\partial_X - (i/\pi)\partial_Y)^2 A$ (see Newell & Whitehead 1969), where the scale $Y = \epsilon^{1/2} y$.

Equations (4.5) and (4.6) are precisely those found in Chen & Davis (1999) who examined the effect of flow on the onset of morphological instability and can be extended to three dimensions as in Chen & Davis (2000).

4.1. *Two-dimensional rolls, $\theta = 0$*

The amplitude equations (4.5) and (4.6) can be used near the critical Rayleigh number to determine the evolution of the mushy-layer convection. Equation (4.5) describes the evolution of disturbances with an axis at an angle to the axis of the weak background flow. For oblique rolls, the essential character of the solutions can be found by considering (4.5) with $\cos\theta = 1$, in which case the equations take the form

$$\frac{\partial A}{\partial \tau'} = 2A_{XX} + (r - is\sin\alpha X)\, A + \lambda A|A|^2, \tag{4.7}$$

with a suitable rescaling of time $\tau = \tau'\left(\Omega - 2S/C^2\Omega\right)$ and with $r = 2\pi R_2 \Omega^{1/2}$, $s = 2\pi^2 K_1 P/C\Omega^{1/2}$ and λ is the coefficient of $|A|^2 A$ in (4.7). The linear stability of this equation has been studied carefully in Chen & Davis (1999) where it is noted that the equation is in parametric excitation form. By considering normal mode

https://doi.org/10.1017/jfm.2011.117 Published online by Cambridge University Press

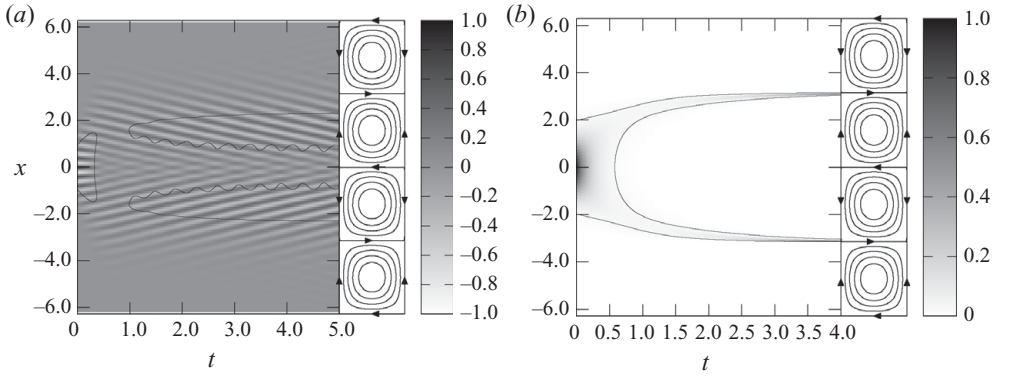


FIGURE 3. (*a*) This figure shows the evolution of the amplitude A (grey-scale) of two-dimensional roll convection as governed by (4.7) with parameters $\alpha = 1$, $s = 10$, $r = 2.5$ and $\lambda = -2$. The figure shows an evolution from an initial Gaussian profile in the amplitude, showing a localisation of an envelope of travelling wave at locations where the background flow is strongest. The line is a contour of constant amplitude, the rolls are tilted, implying travelling waves in the localised envelope. (*b*) The evolution of the amplitude A (grey-scale) of longitudinal rolls from an initial Gaussian hump, as governed by (4.10) with parameters $\alpha = 1$, $s' = 1$, $r = -3$ and $\lambda = 0$. An initial patch of convection is swept to locations in which the background upflow is greatest. The line is a contour of constant amplitude.

solutions $A = A_0\, \mathrm{e}^{(\sigma + \mathrm{i}\omega)t}$ we can search for solutions to the linearised (4.7) using

$$A_0 = \sum_n a_n\, \mathrm{e}^{\mathrm{i}\alpha n X} \tag{4.8}$$

from which we derive the following:

$$\sum_n \mathrm{e}^{\mathrm{i}\alpha n X} \left(-n^2\alpha^2 a_n + \frac{s}{2}\left(a_{n-1} - a_{n+1}\right)\right) = \sum_n \mathrm{e}^{\mathrm{i}\alpha n X} \left(\sigma - r + \mathrm{i}\omega\right) a_n. \tag{4.9}$$

By taking a subset of the a_n say for $n \leqslant N$ for some choice of N, we can approximate both the eigenvalues $\sigma - r + \mathrm{i}\omega$ and the eigenstates $\{a_n\}$. Such an analysis reveals that for both harmonic and subharmonic solutions, the critical Rayleigh number increases for non-zero s and the marginally stable solutions are composed of packets of travelling wave solutions whose amplitude is greatest at those locations where the horizontal flow is strongest. For a detailed discussion on the types of solutions see Chen & Davis (1999). The parameter s scales with the product $K_1 P$, which measures the degree to which the permeability is altered by the background flow. As $|s|$ increases, travelling wave solutions appear that remain localised at points where the horizontal background flow is greatest. The critical Rayleigh number increases with increasing flow strength, in agreement with the results of Neufeld & Wettlaufer (2008) who found that horizontal flow stabilised the mush-mode of convection when the roll axis was perpendicular to the direction of flow, at least for low flow rates. Neufeld & Wettlaufer (2008) also found that the marginally stable modes are travelling wave solutions. Whether the travelling wave nature of the weakly nonlinear convection is inherited by chimneys localised in this way would require further analysis, but the results suggest that this is likely the result of this mechanism of localisation. Figure 3 shows a simulation of the amplitude equations (4.7). Equation (4.7) was solved on a periodic domain using centred differences for the spatial derivatives and an explicit time step, chosen so that the integration is stable. The roll's structure, modulated by

https://doi.org/10.1017/jfm.2011.117 Published online by Cambridge University Press

the amplitude A, is shown in figure 3(a). The figure shows the evolution of a patch of convection as it is localised by the weak background flow in the regions where the horizontal component of the background flow is the largest, the localised packets are composed of travelling wave solutions as indicated by the fact that the stripes are sloped.

4.2. *Longitudinal rolls, $\theta = \pi/2$.*

In the case of longitudinal rolls, (4.6) can be solved exactly using the method of characteristics. It is an equation of the form

$$\frac{\partial A}{\partial \tau'} = rA - 4s'\alpha \cos(\alpha X)\, A - s' \sin(\alpha X) \frac{\partial A}{\partial X} + \lambda A^3, \tag{4.10}$$

where r, λ and τ' are as in (4.7) and $s' = 2\pi\alpha K_1 P / C\Omega^{1/2}$. The characteristics are easily found and the equation along characteristics is a Bernoulli equation for the amplitude which can be transformed to a linear equation and solved to give

$$A(\tau') = A_0(X_0) \exp\left(\int_0^{\tau'} f(u)\, \mathrm{d}u \right) \left[1 - 2A_0(X_0)^2 \lambda \int_0^{\tau'} \exp\left(2 \int_0^u f(v)\, \mathrm{d}v \right) \mathrm{d}u \right]^{-1/2} \tag{4.11}$$

$$f(u) = r - 4\alpha s' \frac{1 - \tan^2(\alpha X_0/2)\, \mathrm{e}^{2s'\alpha u}}{1 + \tan^2(\alpha X_0/2)\, \mathrm{e}^{2s'\alpha u}}. \tag{4.12}$$

The initial conditions are $A(X_0, 0) = A_0(X_0)$. The integrals in (4.11) can be performed exactly. Figure 3 shows the evolution of the amplitude of longitudinal rolls using the exact solution given in (4.11) and (4.12). Figure 3 shows the localisation of mushy layer convection in *regions of upflow in the background flow*. The critical Rayleigh number r *decreases* with s' for this configuration (see Chen & Davis 1999). If the parameter r is above a critical $\sim -s'$ the amplitude grows exponentially, if $\lambda < 0$ then the amplitude saturates and the form of the solution is one of the constant amplitude in a region of size $l(\tau')$ centred at points of upflow. In the absence of any term to regularise the solution then $l(\tau') \to 0$ as $\tau' \to \infty$ (Chen & Davis 1999). For $\lambda > 0$ and r greater than a critical value, the amplitude grows without limit (in the absence of a higher order regularising term). Such concentration of the weakly nonlinear convection would be expected to lead to a localised chimney solution. This weakly nonlinear analysis, however, fails if the amplitude becomes too large and the solid fraction is driven to zero, as chimneys form and alter the dynamics of the mushy layer considerably.

We should treat the results here as an indication that a weak background flow can localise convection in a mushy layer to such an extent that we expect the initial evolution of chimneys as they are born through weakly nonlinear interactions, to be swept by the background flow to locations where the upflow is greatest. This makes physical sense as at these locations the permeability is higher (and thus resistance to flow is reduced) due to dissolution by the background upflow and so we would expect to find more vigorous convection in these locations as opposed to others. As found by Chen & Davis (1999), the most unstable form of rolls is for $\theta = \pi/2$ (longitudinal rolls), and it is these rolls that localise where the upward background flow is greatest.

https://doi.org/10.1017/jfm.2011.117 Published online by Cambridge University Press

5. Conclusion

In this paper, we have shown that the introduction of a background flow leads to the localisation of convection, depending on the orientation of the roll axis relative to the direction of the background flow. We distinguish two cases; the first is when the roll axis makes an angle θ (with $|\theta - \pi/2| \gg \epsilon$) with the roll axis of the large-scale background flow, these oblique rolls are stabilised by the background flow and convection is localised where the horizontal component of the background flow is greatest (not near walls) and is composed of travelling-wave solutions. The parameter that determines the degree of this effect is the product $K_1 P$, that is the product of the strength of the background flow P and the degree to which small variations in porosity affect the permeability K_1.

When the axis of convective rolls is perpendicular to that of the background flow ($\theta = \pi/2$), the effect of the background flow is to localise the convection at positions where the upward component of the background flow is greatest. The change in critical Rayleigh number is again proportional to the combination $K_1 P$. For these longitudinal rolls, the effect is to destabilise the mush relative to the case with no background flow. As the effect of the background flow is to destabilise the mush, we would expect to see longitudinal rolls develop in favour of two-dimensional rolls and for the convection to be localised where the upflow is greatest.

In general, weak and slowly varying background flow in a container will not take the form of simple rolls. It is expected that the local wave-vector of the mush-mode of convection responds to the background flow and orients itself relative to this background flow. A careful study of the effects of wave-vector reorientation would be an interesting extension of this work.

We acknowledge AFOSR (Air Force Office of Scientific Research) MEANS (Materials Engineering for Affordable New Systems) grant no. FA9550-05-1-0089 for partial support.

REFERENCES

Amberg, G. & Homsy, G. M. 1993 Nonlinear analysis of buoyant convection in binary solidification with application to channel formation. *J. Fluid Mech.* **252**, 79–98.

Anderson, D. M. & Worster, M. G. 1995 Weakly nonlinear analysis of convection in mushy layers during the solidification of binary alloys. *J. Fluid. Mech.* **302**, 307–331.

Chen, Y.-J. & Davis, S. H. 1999 Directional solidification of a binary alloy into a cellular convective flow: localised morphologies. *J. Fluid Mech.* **395**, 253–270.

Chen, Y.-J. & Davis, S. H. 2000 Flow-induced patterns in directional solidification: localised morphologies in three-dimensional flows. *J. Fluid Mech.* **421**, 369–380.

Chung, A. A. & Chen, F. 2000 Onset of plume convection in mushy layers. *J. Fluid Mech.* **408**, 53–82.

Fowler, A. C. 1985 The formation of freckles in binary alloys. *IMA J. Appl. Math.* **35**, 159–174.

Giamei, A. F. & Kear, B. H. 1970 On nature of freckles in nickel base superalloys. *Metallurgical Trans.* **1** (8), 2185–2192.

Hills, R. N., Loper, D. E. & Roberts, P. H. 1983 A thermodynamically consistent model of a mushy zone. *Q. J. Mech. Appl. Math.* **36**, 505–539.

Impey, M. D., Riley, D. S. & Winters, K. H. 1990 The effect of sidewall imperfections on pattern formation in lapwood convection. *Nonlinearity* **3**, 197–230.

Katz, R. F. & Worster, M. G. 2008 Simulation of directional solidification, thermochemical convection, and chimney formation in a Hele-Shaw cell. *J. Comput. Phys.* **227** (23), 9823–9840.

https://doi.org/10.1017/jfm.2011.117 Published online by Cambridge University Press

Madison, J., Spowart, J. E., Rowenhorst, D. J., Fiedler, J. & Pollock, T. M. 2008 Characterization of three-dimensional dendritic structures in nickel-base single crystals for investigation of defect formation. In *Superalloys Conf. Proc.*, Champion, PA, pp. 881–888.

Mullins, W. W. & Sekerka, R. F. 1964 Stability of a planar interface during solidification of a binary alloy. *J. Appl. Phys.* **35**, 444–451.

Neufeld, J. A. & Wettlaufer, J. S. October 2008 Shear-enhanced convection in a mushy layer. *J. Fluid Mech.* **612**, 339–361. .

Newell, A. C. & Whitehead, J. A. 1969 Finite bandwidth, finite amplitude convection. *J. Fluid Mech.* **38**, 279–303.

Schulze, T. P. & Worster, M. G. Weak convection, liquid inclusions and the formation of chimneys in mushy layers. *J. Fluid Mech.* **388**, 197–215.

Worster, M. G. 1997 Convection in mushy layers. *Annu. Rev. Fluid Mech.* **29**, 91–122.

Worster, M. G. 1992 Instabilities of the liquid and mushy regions during solidification of alloys. *J. Fluid Mech.* **237**, 649–669.

https://doi.org/10.1017/jfm.2011.117 Published online by Cambridge University Press